



ELSEVIER

Contents lists available at [ScienceDirect](https://www.sciencedirect.com)

Mechanical Systems and Signal Processing

journal homepage: www.elsevier.com/locate/ymssp

Short communication

Size effect in ultrasensitive micro- and nanomechanical mass sensors

Hossein Darban

Institute of Fundamental Technological Research, Polish Academy of Sciences, Pawińskiego 5B, 02-106 Warsaw, Poland

ARTICLE INFO

Communicated by Antonino Morassi

Keywords:

Size dependency
Small scale resonator
Mass detection
Frequency shift

ABSTRACT

The size dependent free transverse vibration of the micro- and nanocantilever mass sensors is studied. The general case of a sensor with an arbitrary number of attached particles is considered. The domain is divided into different segments at the cross-sections where the particles are located, and the displacement fields are described based on the Bernoulli-Euler beam theory. The size effect is introduced into the formulation by assuming the constitutive equation of the stress-driven nonlocal theory of elasticity. The eigenvalue problem is generated by solving the equation of motion in each segment of the sensor and imposing the variationally consistent and higher-order constitutive boundary and continuity conditions. The natural frequencies and their sensitivity to the attachment of a small mass are analyzed analytically. It is shown that the frequency shifts resulting from attachment of a small mass can be explicitly defined as a function of the frequency and mode shape of the unloaded sensor. The model is used to numerically study the natural frequencies of sensors loaded by one to three particles. Comprehensive results are presented on the effect of the size dependency on the frequency shifts of the first four modes of vibration. It is revealed that neglecting the size effect may result in wrong detections of the masses of the attached particles.

1. Introduction

Micro- and nanoelectromechanical systems (MEMS and NEMS) are important devices with many applications in different fields of science and technology. Miniaturized sensors are one of the basic components of MEMS and NEMS. In the case of mass detection, the sensor is usually a cantilever micro- or nanobeam. The cantilever-based mass sensors can detect ultrasmall biological and chemical entities with high resolutions [1]. The mass detection in these devices is based on the natural frequency shifts after the attachment of the entities. Experiments on the free transverse vibration of micro- and nanomechanical mass sensors have been conducted in several works, but often without the consideration of size dependency. Many of these experimental investigations are discussed in the seminal review articles in [1,2] as well as the recent ones in [3,4]. It is well-known that the structural response of small scale beams is size dependent. Therefore, it is necessary to account for the size effect in the design and modeling of the micro- and nanomechanical mass sensors.

Although the atomistic models (e.g. [5]) can accurately simulate the mechanical response of the micro- and nanobeams, they are complex in formulation and computationally expensive in implementation. One efficient methodology for capturing the size dependency in the structural response of the miniaturized beams is based on the strain-driven nonlocal theory proposed by Eringen [6,7], which belongs to the nonclassical continuum mechanics-based theories. Unlike the beam theories based on the classical continuum

E-mail address: hdarban@ippt.pan.pl.

<https://doi.org/10.1016/j.ymssp.2023.110576>

Received 31 January 2023; Received in revised form 26 May 2023; Accepted 28 June 2023

Available online 4 July 2023

0888-3270/© 2023 The Author(s). Published by Elsevier Ltd. This is an open access article under the CC BY license (<http://creativecommons.org/licenses/by/4.0/>).

mechanics which employ local constitutive relations, the constitutive equations of the strain-driven beam theories have a nonlocal nature. For instance, when dealing with the Bernoulli-Euler beam formulation, the bending moment at each cross-section depends on the elastic curvature of all the cross-sections of the beam. The dependency is defined through a convolution integral in terms of a kernel function, which weights the contributions of the long-range interactions. The nonlocal formulations based on Eringen’s theory are used by many scientists to study the size dependent behavior of miniaturized structures, e.g., [8,9]. Assuming a special class of kernels, the integral form of the nonlocal constitutive equation can be converted into a differential form subjected to a set of higher-order constitutive boundary conditions in terms of the bending moment. These higher-order boundary conditions may be in contrast to the equilibrium conditions in some cases, such as a micro- or nanocantilever subject to a transverse end load [10]. An innovative idea, namely the stress-driven nonlocal theory, is proposed in [11] to overcome the ill-conditioning of the strain-driven beam theories by switching the role of the bending moment and elastic curvature in the nonlocal constitutive law. Therefore, the beam formulations based on the stress-driven nonlocal theory are always well-posed since their constitutive boundary conditions are in terms of the elastic curvature and do not contradict the global equilibrium of the beam. The stress-driven beam models predict that the beam becomes stiffer as its dimensions reduce, which is in agreement with the experimental observations in [12]. In [13,14], the applications of the stress-driven nonlocal theory of elasticity are extended to the problems with internal discontinuities, e.g., the miniaturized beams with edge cracks, loading discontinuities, or attached masses. For this purpose, the beam is divided into different segments at the cross-sections where the discontinuities are located and a set of mathematically consistent higher-order continuity conditions associated with the integral form of the constitutive equation are derived. These constitutive continuity conditions are used in [15,16] to study fracture problems in nanobeams, and in [13] and [17] to study the free transverse vibration and buckling of the miniaturized cracked beams.

The problem of size dependent vibration of the small scale mass sensors has been studied in several papers using the nonlocal elasticity theories, e.g. in [18]. A nonlocal Bernoulli-Euler beam model is used in [19] to study the effect of the distributed added mass on the natural frequencies of the carbon nanotube-based mass sensors. In [20], a nonlocal Kirchhoff-Love plate theory is used to study the frequency shifts of a single-layered graphene sheet due to the attachment of particles in the presence of a magnetic field. The vibration of a carbon nanotube-based mass sensor embedded in the nonlocal elastic foundation is studied in [21] through a nonlocal finite element model. The vibration of nanobeams and nanorods carrying a single point mass [22] and distributed mass [23,24], are studied using the modified strain gradient theory. The strain gradient theory is used in [25] to study Kirchhoff-Love nanoplates with point masses. The coupled axial-flexural vibration of cantilever mass nanosensors is investigated in [26] based on a two-phase local/nonlocal elasticity.

In addition to the facts that the stress-driven theory of nonlocal elasticity always results in a well-posed formulation and overcomes the inconsistent restrictions of Eringen’s theory, the theory has been recently shown in [27] to be able to well model the quasi-static and dynamic tests on the micro- and nanobeams. The applications of the stress-driven theory to the problems of mass sensors are very rare. The author is only aware of the recent work in [28], where the free transverse vibration of a Bernoulli-Euler nanocantilever with a tip point mass immersed in water is investigated. However, several particles can land simultaneously at different positions across the miniaturized sensor in practical applications. Therefore, it is fair to claim that there is a gap in the literature since the stress-driven theory of nonlocal elasticity has not been used previously to thoroughly study the size effect in micro- and nanomechanical mass sensors. This paper is aimed at extending the formulation in [28] to the micro- and nanocantilever mass sensors with multiple attached particles at arbitrary locations. To solve the problem, the sensor is first divided into segments at the cross-sections where the particles are located. Then, the variationally consistent governing equations and boundary and continuity conditions, together with the higher-order constitutive boundary and continuity conditions are solved to define the natural frequencies. Novel insightful results are presented confirming that neglecting size dependency may result in significant errors in mass detection. The shielding and amplification of the effect of the particles on the natural frequencies are also studied. In Sect. 2, the problem definition, assumptions, and model formulation are presented. An analytical formulation is presented in Sect. 3 to assess the natural frequencies and their sensitivity to a small mass. In Sect. 4, the model is applied to micro- and nanocantilever mass sensors with one to three attached particles, and the results are presented and discussed for different cases by varying the effective parameters. The concluding remarks are given in sect. 5.

2. Problem definition and formulation

Consider a homogeneous isotropic Bernoulli-Euler micro- or nanocantilever mass sensor with a rectangular cross-section under the plane stress conditions, as shown in Fig. 1. The sensor has the length, in-plane thickness and out-of-plane width of L , h , and b . A

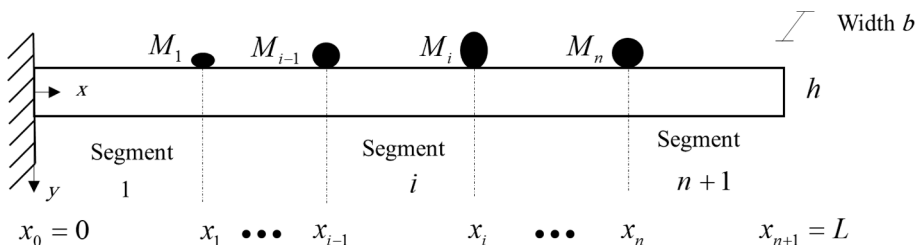


Fig. 1. Micro- or nanocantilever mass sensor with n attached point masses, divided into $n + 1$ segments.

Cartesian coordinate system $x-z$ is placed at the mid-thickness with the origin at the left end of the sensor. Young’s modulus is E and the local elastic compliance $C = 12/(Ebh^3)$. As it is shown in the figure, n different particles, numbered from left to right, with arbitrary masses M_i are attached to the sensor at locations x_i for $i = 1, \dots, n$. The attached particles are assumed to be point masses (i.e. each particle is attached to the sensor at a point rather than over a line) and may represent biological and chemical entities. The eccentricity of the point masses with respect to the axis line of the sensor is neglected. This assumption, which eliminates the effect of the kinetic energy of the attached particles associated with the axial velocities, is common in the literature for studying the vibration of slender mass sensors, e.g., [29]. In addition, it allows for significantly simplifying the formulation since there will be no coupling between the flexural and longitudinal deformations. To study the free transverse vibration of the sensor, the domain is divided into $n+1$ segments at the mass locations. Throughout the formulation, the superscript (i) on the left of a quantity shows the association with the segment i , and $F_{\underbrace{xxx\dots x}_i}$ indicates the i -th derivative of the function F with respect to x . Also, a dot over a function shows the derivative with respect to time, t .

2.1. Problem formulation

The equations governing the vibration of the generic segment i are [30,31]:

- Variationally consistent equation of motion

$${}^{(i)}M_{,xx}^{moment} - I_2 {}^{(i)}\ddot{w}_{,xx} + I_0 {}^{(i)}\ddot{w} = 0 \tag{1}$$

for $i = 1, \dots, n+1$, where ${}^{(i)}w$ is the transverse displacement, and $(I_0, I_2) = (m, mh^2/12)$ with m being the mass per unit length of the cantilever. The bending moment is defined by ${}^{(i)}M^{moment} = \int_A {}^{(i)}\sigma z dA$, where ${}^{(i)}\sigma$ and A are the axial stress of the segment and the cross-section of the cantilever.

- Variationally consistent continuity conditions:

$$\begin{aligned} {}^{(i)}w(x_i, t) &= {}^{(i+1)}w(x_i, t) \\ {}^{(i)}w_{,x}(x_i, t) &= {}^{(i+1)}w_{,x}(x_i, t) \\ {}^{(i)}M^{moment}(x_i, t) &= {}^{(i+1)}M^{moment}(x_i, t) \\ {}^{(i)}M_{,x}^{moment}(x_i, t) - I_2 {}^{(i)}\ddot{w}_{,x}(x_i, t) - M_i {}^{(i)}\ddot{w}(x_i, t) &= {}^{(i+1)}M_{,x}^{moment}(x_i, t) - I_2 {}^{(i+1)}\ddot{w}_{,x}(x_i, t) \end{aligned} \tag{2}$$

for $i = 1, \dots, n$. The four conditions satisfy the continuity of transverse displacement, bending slope, bending moment, and shear force at the cross-sections where the particles are attached.

- Variationally consistent boundary conditions:

$$\begin{aligned} {}^{(1)}w(x=0, t) &= 0 \\ {}^{(1)}w_{,x}(x=0, t) &= 0 \\ {}^{(n+1)}M^{moment}(x=L, t) &= 0 \\ {}^{(n+1)}M_{,x}^{moment}(x=L, t) - I_2 {}^{(n+1)}\ddot{w}_{,x}(x=L, t) &= 0 \end{aligned} \tag{3}$$

The case of a clamped-clamped mass sensor can be modeled by using ${}^{(n+1)}w(x=L, t) = {}^{(n+1)}w_{,x}(x=L, t) = 0$ instead of the last two conditions in Eq. (3). The case of a micro- or nanocantilever mass sensor loaded by one particle at the free end is modeled by Eqs. (1)-(3) for $x_1 = L$. The variationally consistent governing equations (1)-(3) depend on the bending moment and need to be expressed solely in terms of the transverse displacements, ${}^{(i)}w$, using the constitutive equation. Since the mass sensor is a micro- or nanocantilever with size dependent mechanical response, the constitutive equation of the stress-driven nonlocal theory is used [13,14]:

- Differential form of nonlocal constitutive equation

$${}^{(i)}w_{,xx} - L_C^2 {}^{(i)}w_{,xxxx} = C {}^{(i)}M^{moment} \tag{4}$$

for $i = 1, \dots, n+1$, with L_C being the characteristic length parameter.

- Higher-order constitutive boundary and continuity conditions

$$\begin{aligned} {}^{(i)}w_{,xxx}(x_{i-1}, t) &= \frac{1}{L_C} \left[{}^{(i)}w_{,xx}(x_{i-1}, t) - \sum_{k=1}^{i-1} \int_{x_{k-1}}^{x_k} \left(\frac{1}{L_C} e^{-\frac{x_i-\xi}{L_C}} [{}^{(k)}w_{,xx}(\xi, t) - L_C^2 {}^{(k)}w_{,xxxx}(\xi, t)] \right) d\xi \right] \\ {}^{(i)}w_{,xxx}(x_i, t) &= -\frac{1}{L_C} \left[{}^{(i)}w_{,xx}(x_i, t) - \sum_{k=i+1}^{n+1} \int_{x_{k-1}}^{x_k} \left(\frac{1}{L_C} e^{-\frac{x_i-\xi}{L_C}} [{}^{(k)}w_{,xx}(\xi, t) - L_C^2 {}^{(k)}w_{,xxxx}(\xi, t)] \right) d\xi \right] \end{aligned} \tag{5}$$

for $i = 1, \dots, n + 1$. Note that the summation $\sum_a^b F$ is equal to zero if $a > b$. The differential form of the nonlocal constitutive equation (4) and its constitutive boundary and continuity conditions (5) are derived in [13,14] by decomposing the integral form of the constitutive equation of the stress-driven theory. The derivation is purely mathematical and straightforward and can be found in [13,14].

2.2. Equations in terms of displacements

The governing Eqs. (1)-(3) can be written solely in terms of the transverse displacements, ${}^{(i)}w$, using the bending moment definition given by the constitutive equation (4):

$$L_C^2 {}^{(i)}w_{xxxxx} - {}^{(i)}w_{xxxx} + \frac{Cmh^2}{12} \ddot{w}_{xx} - Cm\dot{w} = 0 \tag{6}$$

for $i = 1, \dots, n + 1$,

$$\begin{aligned} &{}^{(i)}w(x_i, t) = {}^{(i+1)}w(x_i, t) \\ &{}^{(i)}w_{,x}(x_i, t) = {}^{(i+1)}w_{,x}(x_i, t) \\ &L_C^2 {}^{(i)}w_{xxxx}(x_i, t) - {}^{(i)}w_{,xx}(x_i, t) = L_C^2 {}^{(i+1)}w_{xxxx}(x_i, t) - {}^{(i+1)}w_{,xx}(x_i, t) \\ &L_C^2 {}^{(i)}w_{xxxxx}(x_i, t) - {}^{(i)}w_{,xxx}(x_i, t) + \frac{Cmh^2}{12} {}^{(i)}\ddot{w}_{,x}(x_i, t) + CM_i {}^{(i)}\ddot{w}(x_i, t) = \\ &L_C^2 {}^{(i+1)}w_{xxxxx}(x_i, t) - {}^{(i+1)}w_{,xxx}(x_i, t) + \frac{Cmh^2}{12} {}^{(i+1)}\ddot{w}_{,x}(x_i, t) \end{aligned} \tag{7}$$

for $i = 1, \dots, n$, and

$$\begin{aligned} &{}^{(1)}w(x = 0, t) = 0 \\ &{}^{(1)}w_{,x}(x = 0, t) = 0 \\ &L_C^2 {}^{(n+1)}w_{xxxx}(x = L, t) - {}^{(n+1)}w_{,xx}(x = L, t) = 0 \\ &L_C^2 {}^{(n+1)}w_{xxxxx}(x = L, t) - {}^{(n+1)}w_{,xxx}(x = L, t) + \frac{Cmh^2}{12} {}^{(n+1)}\ddot{w}_{,x}(x = L, t) = 0 \end{aligned} \tag{8}$$

The equations of motion (6) subjected to the variationally consistent continuity and boundary conditions (7) and (8), together with the constitutive boundary and continuity conditions (5) govern the size dependent free transverse vibration of the loaded miniaturized sensor.

2.3. Solution technique

The equation of motion (6) can be decomposed into a harmonic time-dependent and a spatial differential equation using the separation of variables technique and assuming ${}^{(i)}w = \theta(t) {}^{(i)}\psi(x)$:

$$\begin{aligned} &\ddot{\theta}(t) = -\omega^2\theta(t) \\ &L_C^2 {}^{(i)}\psi_{xxxxx} - {}^{(i)}\psi_{xxxx} + \omega^2 \left[Cm {}^{(i)}\psi - \frac{Cmh^2}{12} {}^{(i)}\psi_{,xx} \right] = 0 \end{aligned} \tag{9}$$

for $i = 1, \dots, n + 1$. The solution to the harmonic time-dependent equation is, $\theta(t) = b_1 \sin(\omega t) + b_2 \cos(\omega t)$, with b_1 and b_2 unknown constants to be determined by imposing suitable initial conditions. The spatial equation can be represented in a dimensionless form using the following dimensionless parameters:

$${}^{(i)}\bar{\psi} = \frac{{}^{(i)}\psi}{L}; \bar{x} = \frac{x}{L}; \bar{h} = \frac{h}{L}; \bar{\omega} = \omega L^2 \sqrt{Cm}; \bar{M}_i = \frac{M_i}{mL}; \lambda = \frac{L_C}{L} \tag{10}$$

as:

$$\lambda^2 {}^{(i)}\bar{\psi}_{xxxxx}(\bar{x}) - {}^{(i)}\bar{\psi}_{xxxx}(\bar{x}) + \bar{\omega}^2 \left[{}^{(i)}\bar{\psi}(\bar{x}) - \frac{\bar{h}^2}{12} {}^{(i)}\bar{\psi}_{xx}(\bar{x}) \right] = 0 \tag{11}$$

for $i = 1, \dots, n + 1$. Similarly, the dimensionless variationally consistent continuity and boundary conditions are obtained from Eqs. (7) and (8) using the dimensionless parameters in Eq. (10) and the harmonic time-dependent differential equation:

$$\begin{aligned}
 & {}^{(i)}\bar{\psi}(\bar{x}_i) = {}^{(i+1)}\bar{\psi}(\bar{x}_i) \\
 & {}^{(i)}\bar{\psi}_{,\bar{x}}(\bar{x}_i) = {}^{(i+1)}\bar{\psi}_{,\bar{x}}(\bar{x}_i) \\
 & \lambda^2 {}^{(i)}\bar{\psi}_{,\bar{x}\bar{x}\bar{x}\bar{x}}(\bar{x}_i) - {}^{(i)}\bar{\psi}_{,\bar{x}\bar{x}}(\bar{x}_i) = \lambda^2 {}^{(i+1)}\bar{\psi}_{,\bar{x}\bar{x}\bar{x}\bar{x}}(\bar{x}_i) - {}^{(i+1)}\bar{\psi}_{,\bar{x}\bar{x}}(\bar{x}_i) \\
 & \lambda^2 {}^{(i)}\bar{\psi}_{,\bar{x}\bar{x}\bar{x}\bar{x}}(\bar{x}_i) - {}^{(i)}\bar{\psi}_{,\bar{x}\bar{x}\bar{x}}(\bar{x}_i) - \frac{\bar{\omega}^2 \bar{h}^2}{12} {}^{(i)}\bar{\psi}_{,\bar{x}}(\bar{x}_i) - \bar{M}_i \bar{\omega}^2 \bar{\psi}(\bar{x}_i) = \\
 & \lambda^2 {}^{(i+1)}\bar{\psi}_{,\bar{x}\bar{x}\bar{x}\bar{x}}(\bar{x}_i) - {}^{(i+1)}\bar{\psi}_{,\bar{x}\bar{x}\bar{x}}(\bar{x}_i) - \frac{\bar{\omega}^2 \bar{h}^2}{12} {}^{(i+1)}\bar{\psi}_{,\bar{x}}(\bar{x}_i)
 \end{aligned} \tag{12}$$

for $i = 1, \dots, n$, and

$$\begin{aligned}
 & {}^{(1)}\bar{\psi}(0) = 0 \\
 & {}^{(1)}\bar{\psi}_{,\bar{x}}(0) = 0 \\
 & \lambda^2 {}^{(n+1)}\bar{\psi}_{,\bar{x}\bar{x}\bar{x}\bar{x}}(1) - {}^{(n+1)}\bar{\psi}_{,\bar{x}\bar{x}}(1) = 0 \\
 & \lambda^2 {}^{(n+1)}\bar{\psi}_{,\bar{x}\bar{x}\bar{x}\bar{x}}(1) - {}^{(n+1)}\bar{\psi}_{,\bar{x}\bar{x}\bar{x}}(1) - \frac{\bar{\omega}^2 \bar{h}^2}{12} {}^{(n+1)}\bar{\psi}_{,\bar{x}}(1) = 0
 \end{aligned} \tag{13}$$

Also, the constitutive boundary and continuity conditions given in Eq. (5) are written in the dimensionless form:

$$\begin{aligned}
 & {}^{(i)}\bar{\psi}_{,\bar{x}\bar{x}\bar{x}}(\bar{x}_{i-1}) = \frac{1}{\lambda} \left[{}^{(i)}\bar{\psi}_{,\bar{x}\bar{x}}(\bar{x}_{i-1}) - \sum_{k=1}^{i-1} \int_{\bar{x}_{k-1}}^{\bar{x}_k} \left(\frac{1}{\lambda} e^{\frac{\xi - \bar{x}_{i-1}}{\lambda}} [{}^{(k)}\bar{\psi}_{,\bar{x}\bar{x}}(\xi) - \lambda^2 {}^{(k)}\bar{\psi}_{,\bar{x}\bar{x}\bar{x}\bar{x}}(\xi)] \right) d\xi \right] \\
 & {}^{(i)}\bar{\psi}_{,\bar{x}\bar{x}\bar{x}}(\bar{x}_i) = -\frac{1}{\lambda} \left[{}^{(i)}\bar{\psi}_{,\bar{x}\bar{x}}(\bar{x}_i) - \sum_{k=i+1}^{n+1} \int_{\bar{x}_{k-1}}^{\bar{x}_k} \left(\frac{1}{\lambda} e^{\frac{\bar{x}_i - \xi}{\lambda}} [{}^{(k)}\bar{\psi}_{,\bar{x}\bar{x}}(\xi) - \lambda^2 {}^{(k)}\bar{\psi}_{,\bar{x}\bar{x}\bar{x}\bar{x}}(\xi)] \right) d\xi \right]
 \end{aligned} \tag{14}$$

for $i = 1, \dots, n + 1$.

The dimensionless form of the equations given in Eqs. (11)-(14) define the size dependent free transverse vibration of the miniaturized sensor with multiple attached masses. The solution of equation (11) for the i -th segment of the cantilever depends on six unknown constants. Therefore, the transverse displacement of the miniaturized cantilever with n attached particles can be defined in terms of $6 \times (n + 1)$ unknown constants. The solutions must satisfy $4 \times n$ variationally consistent continuity conditions in Eq. (12), 4 variationally consistent boundary conditions in Eq. (13), and $2 \times (n + 1)$ constitutive boundary and continuity conditions in Eq. (14). The natural frequencies can be defined by solving the resulting eigenvalue problem.

In general, it is difficult to find closed-form solutions for the frequencies of micro- and nanocantilever mass sensors. Nevertheless, an analytical formulation will be presented in the next section, which allows quantification of the natural frequencies and their sensitivity to a small mass. The numerical results will be presented in Sect. 4.

3. Effect of a small mass on frequency shifts

In this section, the frequency shifts induced due to the attachment of a small mass compared to the total mass of the sensor, i.e., $M_1 \ll mL$ at the location \bar{x}_1 , is considered. The case with multiple attached masses can be analyzed similarly and will be investigated elsewhere. The formulation presented in this section is based on the methodology developed in [22,25,32] and can stimulate further investigation on inverse problem of mass identification from frequency shifts associated with the stress-driven nonlocal formulation.

The derivation starts with multiplying the equation of motion (11) by an admissible test function ${}^{(i)}\varphi$ for $i = 1$ and 2 which satisfies the clamped-free boundary conditions, ${}^{(i)}\varphi(\bar{x}_1) = {}^{(i+1)}\varphi(\bar{x}_1)$, and ${}^{(i)}\varphi_{,\bar{x}}(\bar{x}_1) = {}^{(i+1)}\varphi_{,\bar{x}}(\bar{x}_1)$, and integrating the resulting expressions over the entire length of the sensor. Then, applying integration by parts twice on the first and second terms, and once on the last term, result in the following equation:

$$\begin{aligned}
 & \sum_{i=1}^2 \left[\left(\lambda^2 {}^{(i)}\bar{\psi}_{,\bar{x}\bar{x}\bar{x}\bar{x}} - {}^{(i)}\bar{\psi}_{,\bar{x}\bar{x}\bar{x}} - \frac{\bar{\omega}^2 \bar{h}^2}{12} {}^{(i)}\bar{\psi}_{,\bar{x}} \right) {}^{(i)}\varphi - \left(\lambda^2 {}^{(i)}\bar{\psi}_{,\bar{x}\bar{x}\bar{x}\bar{x}} - {}^{(i)}\bar{\psi}_{,\bar{x}\bar{x}} \right) {}^{(i)}\varphi_{,\bar{x}} \right]_{\bar{x}_{i-1}}^{\bar{x}_i} + \\
 & + \sum_{i=1}^2 \int_{\bar{x}_{i-1}}^{\bar{x}_i} \left[\left(\lambda^2 {}^{(i)}\bar{\psi}_{,\bar{x}\bar{x}\bar{x}\bar{x}} - {}^{(i)}\bar{\psi}_{,\bar{x}\bar{x}\bar{x}} \right) {}^{(i)}\varphi_{,\bar{x}\bar{x}} + \bar{\omega}^2 \left({}^{(i)}\bar{\psi} {}^{(i)}\varphi + \frac{\bar{h}^2}{12} {}^{(i)}\bar{\psi}_{,\bar{x}} {}^{(i)}\varphi_{,\bar{x}} \right) \right] = 0
 \end{aligned} \tag{15}$$

Imposing the boundary and continuity conditions of ${}^{(i)}\bar{\psi}$ given in Eqs. (12) and (13), as well as the characteristics of the test function ${}^{(i)}\varphi$ mentioned above, yield:

$$\sum_{i=1}^2 \int_{\bar{x}_{i-1}}^{\bar{x}_i} \left({}^{(i)}\bar{\psi}_{,xx} - \lambda^2 {}^{(i)}\bar{\psi}_{,xxxx} \right) {}^{(i)}\varphi_{,xx} = \bar{\omega}^2 \left[\bar{M}_1 {}^{(1)}\bar{\psi}(\bar{x}_1) {}^{(1)}\varphi(\bar{x}_1) + \sum_{i=1}^2 \int_{\bar{x}_{i-1}}^{\bar{x}_i} \left({}^{(i)}\bar{\psi} {}^{(i)}\varphi + \frac{\bar{h}^2}{12} {}^{(i)}\bar{\psi}_{,x} {}^{(i)}\varphi_{,x} \right) \right] \tag{16}$$

The associated Rayleigh’s quotient is:

$$R(\varphi) = \frac{\sum_{i=1}^2 \int_{\bar{x}_{i-1}}^{\bar{x}_i} \left({}^{(i)}\varphi_{,xx} - \lambda^2 {}^{(i)}\varphi_{,xxxx} \right) {}^{(i)}\varphi_{,xx}}{\bar{M}_1 [{}^{(1)}\varphi(\bar{x}_1)]^2 + \sum_{i=1}^2 \int_{\bar{x}_{i-1}}^{\bar{x}_i} \left([{}^{(i)}\varphi]^2 + \frac{\bar{h}^2}{12} [{}^{(i)}\varphi_{,x}]^2 \right)} \tag{17}$$

and the square of the frequencies are given by:

$$R(\bar{\psi}) = \bar{\omega}^2 = \frac{\sum_{i=1}^2 \int_{\bar{x}_{i-1}}^{\bar{x}_i} \left({}^{(i)}\bar{\psi}_{,xx} - \lambda^2 {}^{(i)}\bar{\psi}_{,xxxx} \right) {}^{(i)}\bar{\psi}_{,xx}}{\bar{M}_1 [{}^{(1)}\bar{\psi}(\bar{x}_1)]^2 + \sum_{i=1}^2 \int_{\bar{x}_{i-1}}^{\bar{x}_i} \left([{}^{(i)}\bar{\psi}]^2 + \frac{\bar{h}^2}{12} [{}^{(i)}\bar{\psi}_{,x}]^2 \right)} \tag{18}$$

The sensitivity of the square of natural frequencies to the small mass \bar{M}_1 can be estimated by taking the derivative of Eq. (18) with respect to \bar{M}_1 . In general, the mode shape changes when the mass is added to the system. Here, the derivative of the mode shape with respect to the mass of the attached particle is not taken into account. This is an acceptable assumption for small masses attached to long sensors and for lower modes of vibrations, as will be shown later in this section (see Fig. 2). In addition, this assumption leads to the solution which is in agreement with the results presented in the literature, e.g., [22,25,32], and allows drawing general conclusions important for inverse problem of mass identification from frequency shifts. Under this assumption, the derivative of Eq. (18) with respect to \bar{M}_1 reads:

$$\frac{\partial \bar{\omega}^2}{\partial \bar{M}_1} = -\bar{\omega}^2 \frac{[{}^{(1)}\bar{\psi}(\bar{x}_1)]^2}{\bar{M}_1 [{}^{(1)}\bar{\psi}(\bar{x}_1)]^2 + \sum_{i=1}^2 \int_{\bar{x}_{i-1}}^{\bar{x}_i} \left([{}^{(i)}\bar{\psi}]^2 + \frac{\bar{h}^2}{12} [{}^{(i)}\bar{\psi}_{,x}]^2 \right)} \tag{19}$$

The relation given in Eq. (19) agrees with the results obtained in [22,25,32], and implies that no frequency can be increased due to the attachment of the mass.

The validity of the results predicted by Eq. (19) is checked against the numerical results obtained by solving the eigenvalue problem defined by Eqs. (11)-(14) for a cantilever micro- or nanosensor with a mass at $\bar{x}_1 = 0.5$. The thickness to length ratio of the sensor is $\bar{h} = 0.1$ and $\lambda = 0.5$. The first three modes of vibration are considered. An error function is defined as:

$$\text{Error (\%)} = 100 \frac{\delta_M \bar{\omega}^2 - \frac{\partial \bar{\omega}^2}{\partial \bar{M}_1}}{\delta_M \bar{\omega}^2} \tag{20}$$

where $\delta_M \bar{\omega}^2 = (\bar{\omega}_{\text{loaded}}^2 - \bar{\omega}_{\text{unloaded}}^2) / \bar{M}_1$, with $\bar{\omega}_{\text{loaded}}^2$ and $\bar{\omega}_{\text{unloaded}}^2$ being the square of natural frequencies of the sensor with and without the attached mass, determined by solving the eigenvalue problem. The remaining term, $\partial \bar{\omega}^2 / \partial \bar{M}_1$, is defined by Eq. (19) using the frequency and mode shape of the loaded sensor obtained from the eigenvalue problem. The values of the Error function are presented in Fig. 2 by reducing the mass of the attached particle, for the first three modes of vibration.

As evident from the figure, the error rapidly decreases when reducing the mass, indicating that for a small mass, the prediction of Eq. (19) converges to the derivative of the square of natural frequencies with respect to the mass, $\lim_{\bar{M}_1 \rightarrow 0} \delta_M \bar{\omega}^2$. Additionally, the results in Fig. 2 demonstrate that the accuracy of Eq. (19) is higher for the lower modes of vibration.

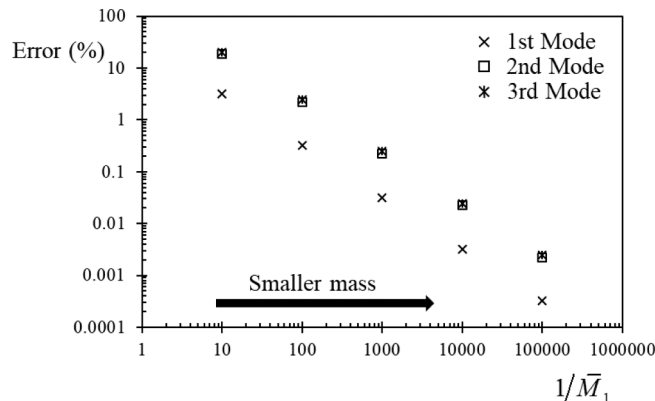


Fig. 2. Error function defined in (20) for different values of attached mass at $\bar{x}_1 = 0.5$. Results are presented for the case with $\bar{h} = 0.1$ and $\lambda = 0.5$.

For a small attached mass, the first order approximation of the natural frequency is obtained by the Taylor series expansion and Eq. (19):

$$\bar{\omega}_{\text{loaded}}^2 = \bar{\omega}_{\text{unloaded}}^2 - \bar{M}_1 \bar{\omega}_{\text{unloaded}}^2 \frac{[(^{(1)}\bar{\psi}(\bar{x}_1))]^2}{\sum_{i=1}^2 \int_{\bar{x}_{i-1}}^{\bar{x}_i} \left([^{(i)}\bar{\psi}]^2 + \frac{\bar{h}^2}{12} [^{(i)}\bar{\psi}_{,x}]^2 \right)} \tag{21}$$

The relation presented in Eq. (21) is derived based on the stress-driven nonlocal theory of elasticity, and emphasizes a significant observation: the frequency shifts induced by a small mass are uniquely determined and can be explicitly expressed in terms of the frequency and mode shape of the unloaded sensor. This is in agreement with the results obtained in [22,25,32] for small-scale structures based on other types of nonclassical continuum mechanics-based theories. Another observation is that when the mass is attached to a node point of the vibration mode, its impact on the frequency disappears. Additionally, since the nonlocal parameter significantly influences the frequency and mode shape of the unloaded sensor (see for instance [13]), it also affects the frequency shifts caused by the attachment of particles. The formula depicted in Eq. (21) serves as the starting point for addressing the inverse problem of mass identification, which will be explored in future studies.

4. Results and discussion

The formulation presented in Sect. 2 is used to investigate how size dependency affects the accuracy of the micro- and nanocantilever mass sensors. Cantilever sensors with one to three attached particles are considered under the assumption that the presence of the attached particles does not change Young’s modulus of the sensor. The effects of the masses and locations of the attached particles and the nonlocal parameter on the natural frequencies are investigated, also for higher modes of vibrations. The shielding/amplification effects of the particles on the natural frequencies, which are controlled by the mass and spacing of the attached entities, are also studied.

4.1. Sensor with single particle attachment

To understand the effect of the size dependency on the accuracy of the miniaturized mass sensors, the frequency percentage changes of the first four modes of vibration due to the attachment of a mass with $\bar{M}_1 = 0.1$ at different locations are shown in Fig. 3 for the case with $\bar{h} = 0.1$ by varying the nonlocal parameter, λ . Generally, if the curve corresponding to $\lambda = 0$ is placed below the curves with $\lambda \neq 0$, neglecting the size dependency results in the underestimation of the attached mass, and if the curve for $\lambda = 0$ is placed above the curves

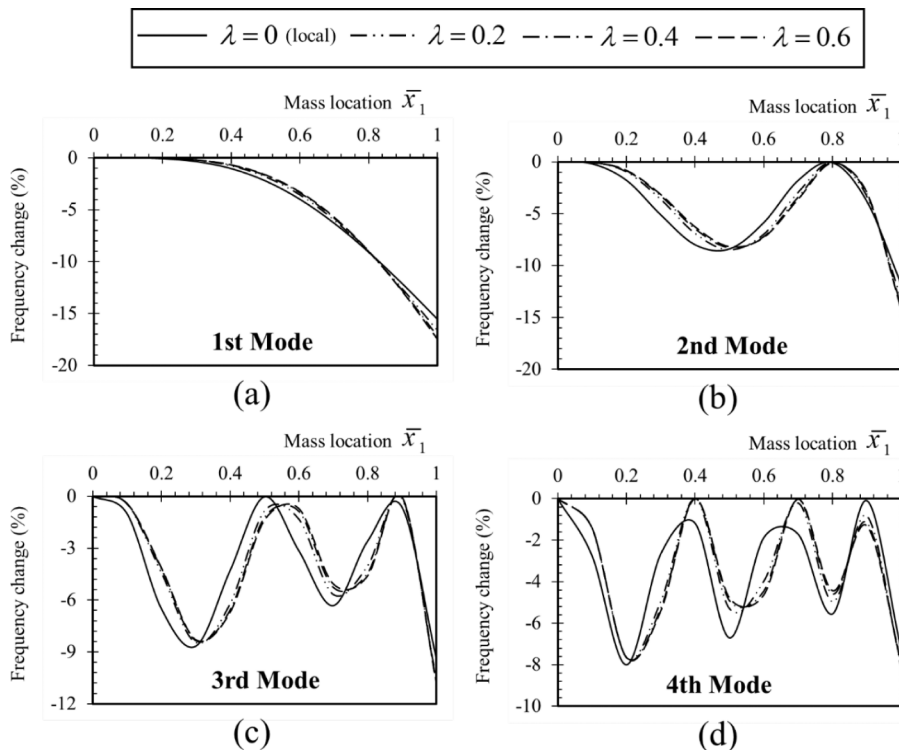


Fig. 3. Changes in the frequency of the (a) first, (b) second, (c) third, and (d) fourth mode of vibration in a micro- or nanocantilever sensor due to the attachment of a mass with $\bar{M}_1 = 0.1$ at different locations. The results are presented for $\bar{h} = 0.1$ by varying the nonlocal parameter, λ .

above the other curves, then neglecting the size effect results in the overestimation. In the first mode of vibration, neglecting the size dependency results in the underestimation and the overestimation of the mass attached at locations within the intervals approximately equal to, respectively, $\bar{x}_1 \leq 0.8$ and $\bar{x}_1 > 0.8$. The frequency shifts of the first mode of vibration due to the presence of the mass at $\bar{x}_1 = 0.8$ are almost independent of the size dependency. This can be seen in Fig. 3(a) where all the curves virtually intersect at $\bar{x}_1 = 0.8$. The behavior is more complex for the second, third, and fourth modes of vibration, and is controlled by the location of the attached mass. For instance, if the particle is attached at approximately $\bar{x}_1 \leq 0.5$ and $0.5 < \bar{x}_1 < 0.8$, neglecting the size dependency results in, respectively, the underestimation and the overestimation of the mass based on the second mode of vibration. It can be seen in Fig. 3(d) that for a size dependent sensor, the presence of a mass at $\bar{x}_1 = 0.4$ or 0.7 has almost no effect on the natural frequency of the fourth mode of vibration.

4.2. Sensor with multiple particles attachment

The formulated model can be readily applied to investigate the natural frequencies of micro- and nanocantilever mass sensors with multiple particles attachment and to study the shielding or amplification of the effect of the particles on the natural frequencies. This behavior is controlled by the mass and spacing of the particles. The cases of sensors with two and three attached particles are considered in this section.

The curves in Fig. 4 correspond to the dimensionless fundamental natural frequencies of a cantilever micro- or nanosensor with two attached masses at $\bar{x}_1 = 0.8$ and $\bar{x}_2 = 1$, and $\bar{h} = 0.1$. The results are presented for the local and nonlocal sensors by varying the dimensionless mass of the first particle, \bar{M}_1 , while the mass of the second particle is kept constant and equal to 0, 0.2, and 0.4. In the absence of the second mass, $\bar{M}_2 = 0$, the fundamental natural frequency is dependent on the mass of the first particle, and reduces by increasing \bar{M}_1 . However, the effect of the first mass on the natural frequency is shielded when the second mass is added to the system. The shielding is more highlighted for higher values of the second mass, \bar{M}_2 , and the nonlocal parameter, λ .

The shielding or amplification of the effect of the particles on the natural frequencies depends also on the mode of vibration. This is shown in Fig. 5, where the natural frequencies of the first four modes of vibration of a cantilever micro- or nanosensor with $\lambda = 0.4$, two attached masses at $\bar{x}_1 = 0.7$ and $\bar{x}_2 = 1$, $\bar{h} = 0.1$, and $\bar{M}_1 = 0.05$ are presented. The natural frequencies are normalized with respect to the natural frequencies of the sensor in the absence of the first mass, $\omega_{Single}^{M_2}$. The results are presented by varying the

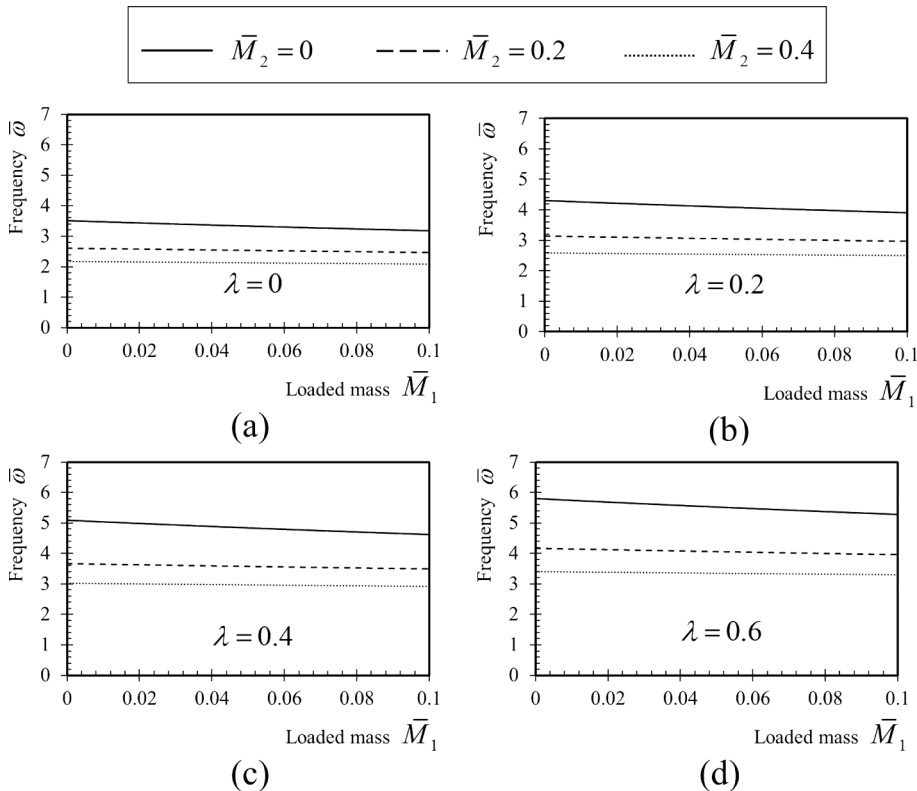


Fig. 4. Dimensionless fundamental natural frequencies of a cantilever micro- or nanosensor with (a) $\lambda = 0$ (local model), (b) $\lambda = 0.2$, (c) $\lambda = 0.4$, and (d) $\lambda = 0.6$, two attached masses at $\bar{x}_1 = 0.8$ and $\bar{x}_2 = 1$, and $\bar{h} = 0.1$. The results are presented by varying the dimensionless mass of the first particle for three cases with the dimensionless mass of the second particle, \bar{M}_2 , equal to 0, 0.2, and 0.4.

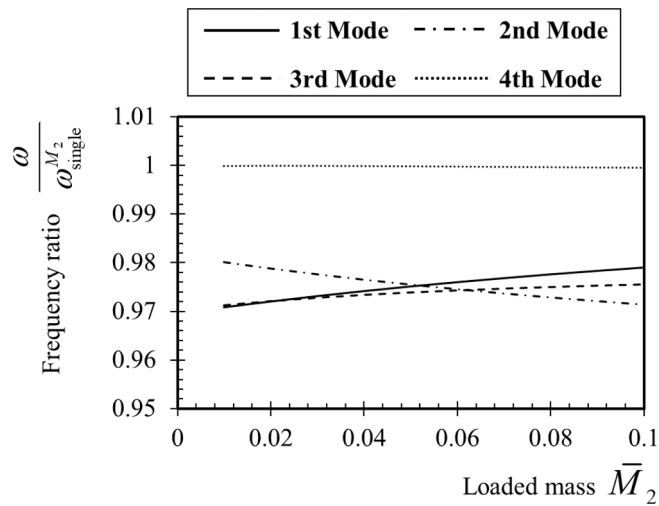


Fig. 5. Dimensionless natural frequencies of the first four modes of vibration of a cantilever micro- or nanosensor with $\lambda = 0.4$, two attached masses at $\bar{x}_1 = 0.7$ and $\bar{x}_2 = 1$, $\bar{h} = 0.1$, and $\bar{M}_1 = 0.05$. The natural frequencies are normalized with respect to the natural frequencies of the sensor in the absence of the first mass. The results are presented by varying the dimensionless mass of the second particle, \bar{M}_2 .

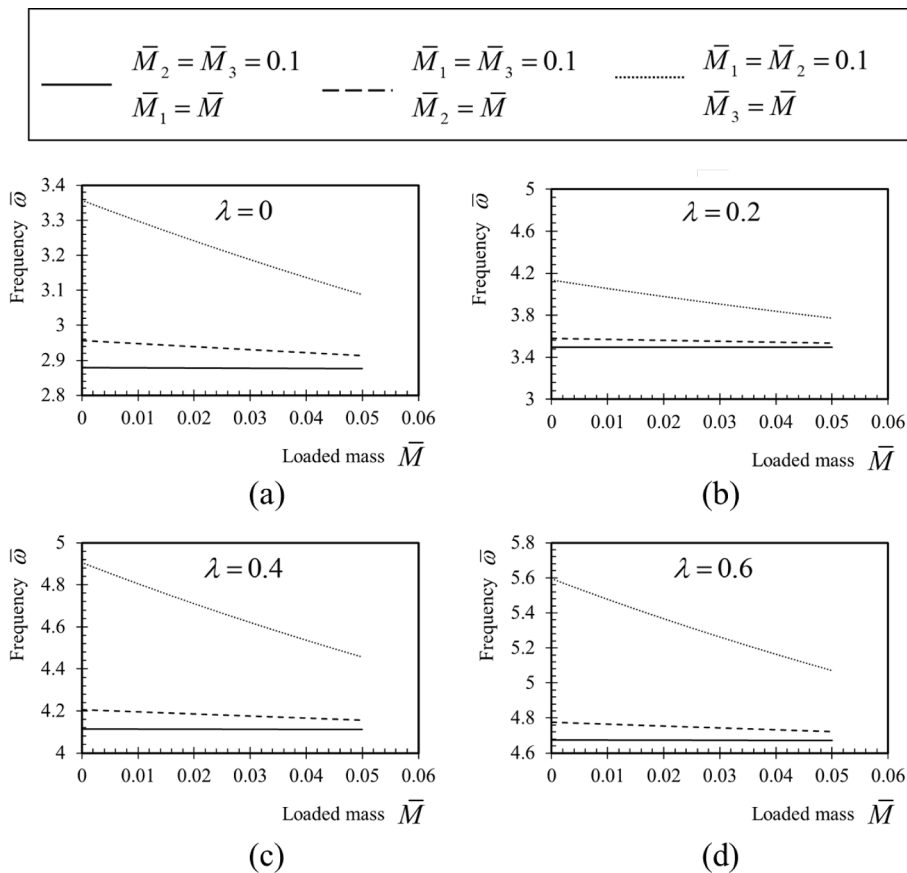


Fig. 6. Dimensionless fundamental natural frequencies of a cantilever micro- or nanosensor with (a) $\lambda = 0$ (local model), (b) $\lambda = 0.2$, (c) $\lambda = 0.4$, and (d) $\lambda = 0.6$, three attached masses at $\bar{x}_1 = 0.3$, $\bar{x}_2 = 0.6$, and $\bar{x}_3 = 1$, and $\bar{h} = 0.1$. The results are presented by varying the dimensionless mass of each particle while the dimensionless masses of other particles are kept constant and equal to 0.1.

dimensionless mass of the second particle, \bar{M}_2 . As can be seen in the figure, the behavior of the sensor is highly dependent on the mode of vibration. For the first and the third mode of vibration, increasing the second mass shields the effect of the first mass on the natural frequency. The shielding phenomenon is more noticeable for the first mode of vibration. The interaction effect on the natural frequency of the second mode of vibration is of an amplification type, where increasing the second mass amplifies the effect of the first mass on the natural frequency. The presence of the first mass at $\bar{x}_1 = 0.7$ has almost no effect on the natural frequency of the fourth mode of vibration for any value of \bar{M}_2 .

The fundamental natural frequencies of a micro- or nanocantilever mass sensor with three attached masses at $\bar{x}_1 = 0.3$, $\bar{x}_2 = 0.6$, and $\bar{x}_3 = 1$, and $\bar{h} = 0.1$ are presented in Fig. 6. The results are presented for the local and nonlocal sensors by varying the dimensionless mass of each particle while the dimensionless masses of other particles are kept constant and equal to 0.1. The figure shows that the effect of the first particle on the natural frequency of the sensor is shielded by the presence of the other particles at further distances (solid lines). Moreover, the presence of the third mass at the free end shields the effect of the second mass on the natural frequency, as the change in the natural frequency due to the change in the mass of the second particle is almost negligible (dashed lines). The shielding of the effects of the first and second particles on the natural frequencies due to the presence of the third particle is more pronounced for the nonlocal sensors. The natural frequency of the mass sensor highly depends on the mass of the third particle and significantly reduces for higher masses (dotted lines). The dependency of the natural frequencies on the mass of the third particle is more noticeable for the sensors with higher values of the nonlocal parameter.

5. Conclusions

The size dependent free transverse vibration of a micro- or nanocantilever sensor loaded by an arbitrary number of attached particles has been studied through the variational approach and the stress-driven nonlocal theory of elasticity. The kinematic field at the segments of the sensor between each two attached particles has been defined using the Bernoulli-Euler beam theory. The natural frequencies have been obtained by solving the variationally consistent governing equations together with the higher-order constitutive boundary and continuity conditions. In cases where the attached particle has a small mass in comparison to the mass of the sensor, a first-order approximation of the natural frequencies has been derived solely based on the frequency and mode shape of the unloaded sensor. This formula, which agrees with previous findings in the literature, provides a foundation for future investigations into the inverse problem of mass identification based on the stress-driven nonlocal theory using minimal frequency data. The formulated model has been applied to numerically obtain the first four natural frequencies of the micro- or nanocantilever mass sensors with one to three attached particles. It has been shown that neglecting the size effect may result in a significant overestimation or underestimation of the mass depending on the location of the particles, and the mode of vibration. For the sensors with multiple attached particles, the model captures the shielding or amplification of the effect of the particles on the natural frequencies. It has been shown that the shielding and amplification effects are generally more highlighted when the size effect is considered in the modeling.

Funding

This research did not receive any specific grant.

Declaration of Competing Interest

The authors declare that they have no known competing financial interests or personal relationships that could have appeared to influence the work reported in this paper.

Data availability

The authors are unable or have chosen not to specify which data has been used.

References

- [1] P.S. Wagoner, H.G. Craighead, Micro- and nanomechanical sensors for environmental, chemical, and biological detection, *Lab Chip* 7 (10) (2007) 1238–1255.
- [2] N.V. Lavrik, M.J. Sepaniak, P.G. Datskos, Cantilever transducers as a platform for chemical and biological sensors, *Rev. Sci. Instrum.* 75 (7) (2004) 2229–2253.
- [3] L. Wei, X. Kuai, Y. Bao, J. Wei, L. Yang, P. Song, M. Zhang, F. Yang, X. Wang, The recent progress of MEMS/NEMS resonators, *Micromachines* 12 (6) (2021) 724.
- [4] V. Pachkawade, Z. Tse, MEMS sensor for detection and measurement of ultra-fine particles, *Eng. Res. Express.* 4 (2) (2022), 022002.
- [5] J.F. Wang, J.P. Yang, L.H. Tam, W. Zhang, Molecular dynamics-based multiscale nonlinear vibrations of PMMA/CNT composite plates, *Mech. Syst. Sig. Process.* 153 (2021), 107530.
- [6] A.C. Eringen, D.G.B. Edelen, On nonlocal elasticity, *Int. J. Eng. Sci.* 10 (3) (1972) 233–248.
- [7] A.C. Eringen, On differential equations of nonlocal elasticity and solutions of screw dislocation and surface waves, *J. Appl. Phys.* 54 (9) (1983) 4703–4710.
- [8] F. Ebrahimi, M.R. Barati, Porosity-dependent vibration analysis of piezo-magnetically actuated heterogeneous nanobeams, *Mech. Syst. Sig. Process.* 93 (2017) 445–459.
- [9] A. Naderi, M. Fakher, S. Hosseini-Hashemi, On the local/nonlocal piezoelectric nanobeams: Vibration, buckling, and energy harvesting, *Mech. Syst. Sig. Process.* 151 (2021), 107432.
- [10] N. Challamel, C.M. Wang, The small length scale effect for a non-local cantilever beam: a paradox solved, *Nanotechnology* 19 (34) (2008), 345703.
- [11] G. Romano, R. Barretta, Nonlocal elasticity in nanobeams: the stress-driven integral model, *Int. J. Eng. Sci.* 115 (2017) 14–27.
- [12] D.C.C. Lam, F. Yang, A.C.M. Chong, J. Wang, P. Tong, Experiments and theory in strain gradient elasticity, *J. Mech. Phys. Solids* 51 (8) (2003) 1477–1508.
- [13] H. Darban, R. Luciano, M. Basista, Free transverse vibrations of nanobeams with multiple cracks, *Int. J. Eng. Sci.* 177 (2022), 103703.

- [14] A. Caporale, H. Darban, R. Luciano, Exact closed-form solutions for nonlocal beams with loading discontinuities, *Mech. Adv. Mater. Struct.* 29 (5) (2022) 694–704.
- [15] H. Darban, F. Fabbrocino, R. Luciano, Size-dependent linear elastic fracture of nanobeams, *Int. J. Eng. Sci.* 157 (2020), 103381.
- [16] S. Vantadori, R. Luciano, D. Scorza, H. Darban, Fracture analysis of nanobeams based on the stress-driven non-local theory of elasticity, *Mech. Adv. Mater. Struct.* 29 (14) (2022) 1967–1976.
- [17] H. Darban, R. Luciano, R. Darban, Buckling of cracked micro- and nanocantilevers, *Acta Mechanica* 234 (2) (2023) 693–704.
- [18] M.A. De Rosa, M. Lippiello, E. Babilio, C. Ceraldi, Nonlocal vibration analysis of a nonuniform carbon nanotube with elastic constraints and an attached mass, *Materials* 14 (13) (2021) 3445.
- [19] M.A. De Rosa, M. Lippiello, H.D. Martin, M.T. Piovan, Nonlocal frequency analysis of nanosensors with different boundary conditions and attached distributed biomolecules: an approximate method, *Acta Mech.* 227 (8) (2016) 2323–2342.
- [20] D. Karličić, P. Kozić, S. Adhikari, M. Cajić, T. Murmu, M. Lazarević, Nonlocal mass-nanosensor model based on the damped vibration of single-layer graphene sheet influenced by in-plane magnetic field, *Int. J. Mech. Sci.* 96–97 (2015) 132–142.
- [21] M. Fakher, S. Rahmani, S. Hosseini-Hashemi, On the carbon nanotube mass nanosensor by integral form of nonlocal elasticity, *Int. J. Mech. Sci.* 150 (2019) 445–457.
- [22] A. Morassi, J. Fernández-Sáez, R. Zaera, J.A. Loya, Resonator-based detection in nanorods, *Mech. Syst. Sig. Process.* 93 (2017) 645–660.
- [23] M. Dilena, M. Fedele Dell’Oste, J. Fernández-Sáez, A. Morassi, R., Zaera: Recovering added mass in nanoresonator sensors from finite axial eigenfrequency data, *Mech. Syst. Sig. Process.* 130 (2019) 122–151.
- [24] M. Dilena, M.F. Dell’Oste, J. Fernández-Sáez, A. Morassi, R. Zaera, Identification of general added mass distribution in nanorods from two-spectra finite data, *Mech. Syst. Sig. Process.* 134 (2019), 106286.
- [25] J. Fernández-Sáez, A. Morassi, L. Rubio, R. Zaera, Transverse free vibration of resonant nanoplate mass sensors: Identification of an attached point mass, *Int. J. Mech. Sci.* 150 (2019) 217–225.
- [26] A. Naderi, S. Behdad, M. Fakher, S. Hosseini-Hashemi, Vibration analysis of mass nanosensors with considering the axial-flexural coupling based on the two-phase local/nonlocal elasticity, *Mech. Syst. Sig. Process.* 145 (2020), 106931.
- [27] H. Darban, R. Luciano, M. Basista, Calibration of the length scale parameter for the stress-driven nonlocal elasticity model from quasi-static and dynamic experiments, *Mech. Adv. Mater. Struct.* (2022) 1–7, <https://doi.org/10.1080/15376494.2022.2077488>.
- [28] R. Barretta, M. Čanadija, F. Marotti de Sciarra, A. Skoblar, Free vibrations of bernoulli-euler nanobeams with point mass interacting with heavy fluid using nonlocal elasticity, *Nanomaterials* 12 (15) (2022) 2676.
- [29] K.H. Low, On the methods to derive frequency equations of beams carrying multiple masses, *Int. J. Mech. Sci.* 43 (3) (2001) 871–881.
- [30] J. Prescott, *Applied elasticity*, Longmans, Green and Company, 1924.
- [31] W. Weaver Jr, S.P. Timoshenko, D.H. Young, *Vibration problems in engineering*, John Wiley & Sons, 1991.
- [32] M. Dilena, M. Fedele Dell’Oste, J. Fernández-Sáez, A. Morassi, R., Zaera: Mass detection in nanobeams from bending resonant frequency shifts, *Mech. Syst. Sig. Process.* 116 (2019) 261–276.